Degradation of Quaternary cinder cones in the Cima volcanic field, Mojave Desert, California

JOHN C. DOHRENWEND *U.S. Geological Survey, 345 Middlefield Road, Menlo Park, California 94025*
STEPHEN G. WELLS *Department of Geology, University of New Mexico, Albuquerque, New Mexico 87131*
BRENT D. TURRIN *U.S. Geological Survey, 345 Middlefield Road, Menlo Park, California 94025*

ABSTRACT

Basaltic cinder cones in the Cima volcanic field record a detailed history of progressive erosion in the arid environment of the eastern Mojave Desert. These cones range in age from ~0.015 m.y. to 1.09 ± 0.08 m.y., as dated by radiocarbon or K-Ar analyses of the youngest lava flows from each cone. Cone heights range from 50 to 155 m, and basal widths range from 400 to 915 m; on younger cones, height/width ratios average 0.17, and crater-width/cone-width ratios average 0.42. The degradational morphology of these cones displays several trends that are closely related to cone age. (1) Crater-width/cone-width ratios decrease from 0.48 on the youngest cone to 0.21 on the oldest cone with a preserved crater. (2) Mean maximum side slopes (Tan S_c) decrease from 0.575 on the youngest cone to an average of 0.41 on the oldest cones studied. (3) Debris-apron-height/cone-height ratios increase from <0.10 on the youngest cone to an average of 0.34 on the oldest cones. (4) Cone drainage evolves from irregularly spaced rills and gullies on the youngest cone to regularly spaced gullies on 0.20- to 0.35-m.y.-old cones to valleys as much as 110 m wide and 10 m deep on cones 0.59 m.y. old and older.

These trends form the basis of an empirical model of cinder-cone degradation in arid environments. This model documents (1) an erosional loss of ~15% of cone volume during the first million years; (2) progressive decline of cone slope (at an average rate of $0.006°/10^3$ yr) and cone height (at an average rate of 2.25 cm/10^3 yr); (3) initial rapid stripping of the loose cinder mantle from upper-cone slopes accompanied by rapid debris-apron formation; and (4) a gradual transition, between 0.25 and 0.6 m.y., from relatively uniform stripping of upper slopes to localized fluvial dissection of both cone slopes and debris apron. This transition is apparently controlled by a concomitant change from diffuse subsurface drainage within the pervious cinder mantle to concentrated surface flow across the heterogeneous assemblage of agglutinate layers, dikes, and ponded flows of the cone interior.

INTRODUCTION

Cinder cones of similar composition and structure frequently occur in large populations. The ages of cones commonly can be determined by ^{14}C or K-Ar methods, and their original morphology can be reconstructed with reasonable accuracy. Cinder cones thus are ideal landforms for quantitative analysis of degradational evolution. Wood (1980a) presented morphometric data for cinder cones from five volcanic fields on three continents, indicating that cone heights, height/width ratios, and average side-slope angles systematically decrease with time. In addition, the degree of cinder-cone degradation has been used qualitatively to provide generalized temporal frameworks for volcanic fields around the world (for example, Kear, 1957—New Zealand; Colton, 1967—Arizona; Scott and Trask, 1971—Nevada; Bloomfield, 1975, and Hasenaka and Carmichael, 1985—Mexico). In recent years, cone morphometry has been used in attempts to analyze eruption styles and to interpret the eruption dynamics of volcanic fields (Bloomfield, 1975; Settle, 1979; Wood, 1980b; Hasenaka and Carmichael, 1985). Long-term degradation of cinder cones, however, has not been used to study the surficial processes that have operated to affect that degradation. This paper quantitatively documents degradational morphologic changes (spanning a period of ~1.1 m.y.) on 11 cinder cones in the Cima volcanic field of southeast California (Fig. 1) and discusses these changes in terms of the types and rates of surficial processes that caused them.

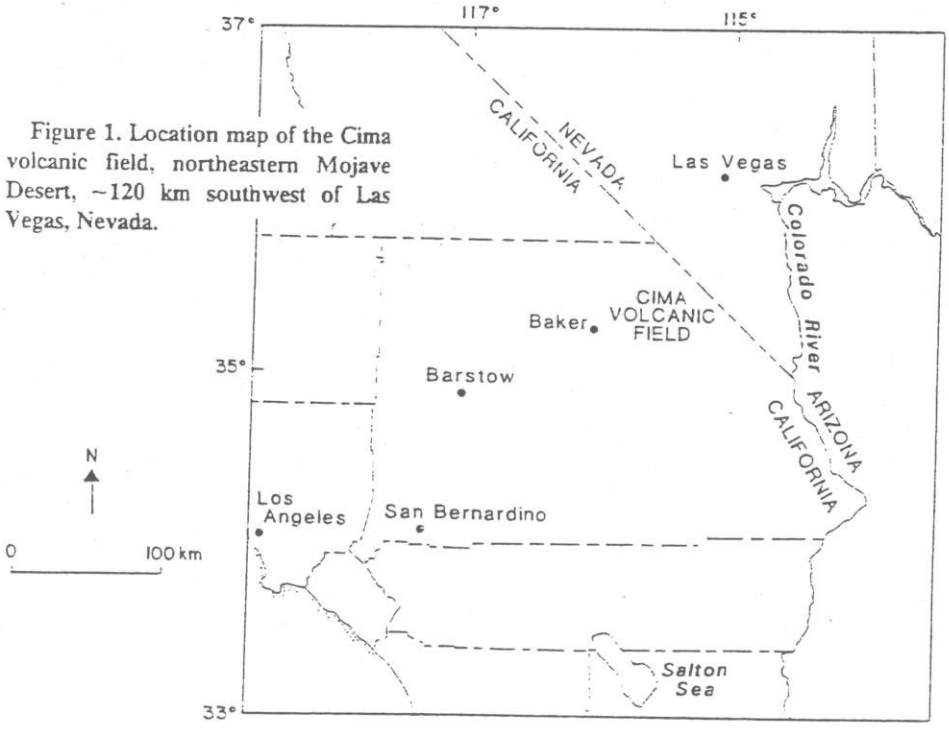

Figure 1. Location map of the Cima volcanic field, northeastern Mojave Desert, ~120 km southwest of Las Vegas, Nevada.

Geological Society of America Bulletin, v. 97, p. 421–427, 7 figs., 5 tables, April 1986.

GENERAL GEOLOGY OF THE CIMA CONES

Morphology

More than 30 cones of Pleistocene age are located in the southern part of the Cima volcanic field (Fig. 2). These cones form a progressive morphologic series from relatively undissected cones to deeply eroded, irregular hills with exposed agglutinate layers and feeder dikes. Mean cone heights range between 50 and 155 m, and mean widths range between 400 and 915 m. The craters surmounting the younger cones are as much as 45 m deep and 330 m wide. On the younger cones, height/width ratios (H_c/W_c) range from 0.15 to 0.19 and average 0.17, crater-width/cone-width ratios (W_{cr}/W_c) range from 0.32 to 0.48 and average 0.42, and maximum side-slope angles (S_c) range from 26° to 30° and average ~28.5°. These values are similar to values of the same morphometric parameters determined for cinder cones on Mauna Kea Volcano, Hawaii (Porter, 1972), and for younger cones in the San Francisco volcanic field, Arizona (Wood, 1980a).

Geology

Cinders, bombs, agglutinate, and flow rock (ranging in composition from alkali olivine basalt to basanite) are the primary constituents of the Pleistocene cones in the Cima field. The cinders, although unconsolidated, are generally tightly packed in well-defined, moderately to well-sorted strata oriented subparallel to outer cone slopes. They vary in size from coarse sand to irregular cobble-sized clasts as much as 15 cm in maximum dimension. The bombs, generally fusiform to approximately equant in shape, range from a few centimetres to as much as 2 m in length. Although many bombs have been broken into cobble- and boulder-sized fragments, unbroken bombs are common even on older cones. Thick mantles of cinders and bombs typically cover the crest and outer slopes of the less degraded cones. Beneath these unconsolidated mantles, layers and irregular masses of agglutinate or welded spatter as much as several metres thick are commonly intercalated within the cinder layers. These agglutinate masses are frequently exposed in the deep gullies and small valleys of the more degraded cones, and they commonly form discontinuous collars around the crests and upper flanks of these cones. In combination with remnants of feeder dikes, rootless flows, and crater-ponded lavas, the agglutinate forms relatively impervious and erosion-resistant cores within most cones.

Tephra rings flank four closely spaced vents (vents H, I, M, and O in Fig. 2) in the south-central part of the Cima field. Exposures within these rings reveal low-angle cross-bedding and antidune structures characteristic of base-surge deposits. Owing to significant differences in clast-size distribution, bedding structure, and

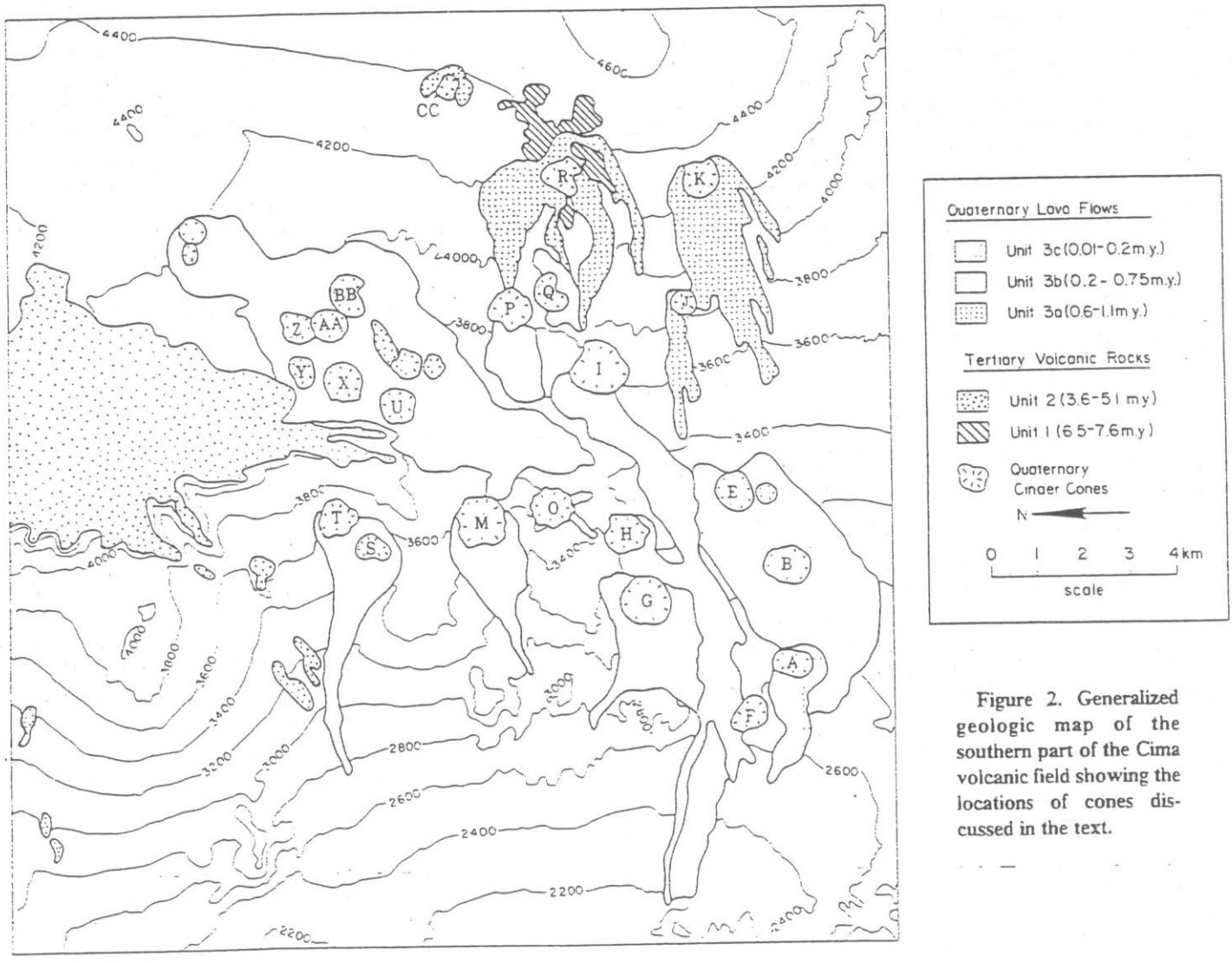

Figure 2. Generalized geologic map of the southern part of the Cima volcanic field showing the locations of cones discussed in the text.

original constructional form, cones associated with tephra rings were excluded from the morphometric analysis of this study.

Cinder cones are typically constructed by a single eruption, and when activity ceases, it is rare for a second eruption to occur from the same vent (Williams and McBirney, 1979; Wood, 1980a). Detailed K-Ar dating and geomorphic analyses of multiple flows from individual cones in the Cima field indicate, however, that several of the Cima vents have erupted discontinuously over periods of hundreds of thousands of years (Turrin and others, 1984; Wells and others, 1984). On account of this discontinuous style of eruptive activity, determining the age of the youngest constructional form of each cone requires identification and K-Ar dating of the youngest flow associated with that cone.

Cone Ages

The cones and flows of the Quaternary part of the Cima volcanic field range in age from 0.015 to 1.09 m.y. (Table 1). The 0.015-m.y. age of the youngest cone and its associated flow is based on four independent lines of evidence: relative soil development (McFadden and others, 1984), a highly diagnostic paleomagnetic direction (Duane Champion, 1984, oral commun.), rock-varnish chemistry, and ^{14}C dating of rock varnish (Dorn, 1984). Ages for the other ten dated cones were determined by K-Ar analyses of whole-rock samples from the youngest lava flow associated with each cone. Samples were processed according to the procedures described in Dohrenwend and others (1984a) and Turrin and others (1984). The accuracy of these K-Ar ages is supported by several independent lines of evidence. (1) Paleomagnetic polarity measurements of all dated flows are consistent with the latest revision of the paleomagnetic time scale (Harland and others, 1983). (2) Replicate ages for 2 of the younger flows suggest analytic reproducibility within 0.06 m.y. (3) The K-Ar ages accord well with progressive changes in flow-surface morphology (Wells and others, 1984), soil-profile development (McFadden and others, 1984), and rock-varnish chemistry (Dorn, 1984). Because the Cima cones are similar in lithology, structure, and original constructional form and because their ages are more or less uniformly distributed over the past 1.1 m.y., they constitute a precisely dated series of landforms that can be used to measure rates and processes of long-term erosion.

MEASUREMENT OF MORPHOMETRIC PARAMETERS

Morphometric data and morphologic descriptions of the Cima cones are derived from a combination of field-based measurements and observations supported by photogrammetric and photogeologic analyses. The morphometric parameters used to describe the cones are defined in Figure 3. The mean maximum slope angle (S_c) of each cone was determined by averaging 10 to 15 Abney level measurements of maximum slope taken at selected locations around the cone perimeter. Only unbreached slopes were measured. These averages were verified by photogrammetric determinations of maximum slope measured from multiple photographs of cone profiles. At least four different profiles were measured for each cone. Cone width (W_c) and crater width (W_{cr}) were estimated by averaging photogrammetric measurements on 1:20,000-nominal-scale, vertical aerial photographs. (The lower parts of the original cone slopes are buried beneath debris aprons, and so cone perimeters cannot be precisely located but are judged to lie beneath the zone of maximum curvature of the overlying debris apron.) These measurements were calibrated with 1:24,000-scale, 10-m-contour topographic maps. Debris-apron–height (H_a), apron-height/cone-height ratios (H_a/H_c), and apron-slope-length/cone-slope-length ratios (L_a/L_c) were estimated from field measurements and analysis of horizontal photography of cone profiles. Mean dimensions of gullies and small valleys on cone slopes were estimated from field measurements of randomly selected drainage ways on each of six cones. Descriptions of drainage networks were developed from analysis of vertical aerial photographs and verified by field measurements and observations.

Only 11 of the 31 Quaternary cones in the Cima field were selected for morphometric analysis. Of the 20 cones that were not analyzed, 5 are associated with tephra rings, 2 are multiple composites of several vents, and the remainder have not been adequately dated. In most cases, the youngest flows from these undated vents are either too altered or too poorly exposed to yield datable material.

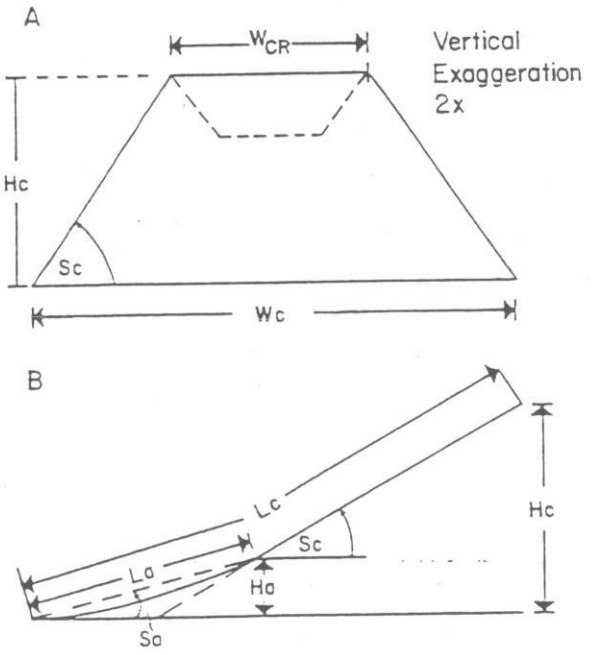

Figure 3. Definition of morphometric parameters. A. Cone cross section showing cone height (H_c), cone-slope angle (S_c), cone width (W_c), and crater width (W_{cr}). Debris apron not shown. Vertical exaggeration 2×. B. Cone-slope cross section showing cone height (H_c), apron height (H_a), cone-slope angle (S_c), mean apron-slope angle (S_a), cone-slope length (L_c), and apron-slope length (L_a). No vertical exaggeration.

CONE DEGRADATION

Slope Morphology

The Cima cones show several progressive changes in morphometry and slope morphology through time (Table 2; Figs. 4 and 5). Cone-height/cone-width ratios (H_c/W_c), crater-width/cone-width ratios (W_{cr}/W_c), and mean maximum slopes (tan S_c) generally decrease with increasing cone age, whereas debris-apron–height/cone-height ratios (H_a/H_c) and apron-slope-length/cone-slope-length ratios (L_a/L_c)

TABLE 1. CIMA VOLCANIC FIELD: CONE AGE DATA

Cone	Age (m.y.)	Age dating method	Magnetic polarity
A	0.015 ± 0.005	^{14}C; CRD*	Normal
U	0.16 ± 0.07	K-Ar	Normal
G	0.22 ± 0.03	K-Ar	Normal
BB	0.33 ± 0.16	K-Ar	Normal
E	0.35 ± 0.04	K-Ar	Normal
J	0.46 ± 0.05	K-Ar	Normal
F	0.59 ± 0.09	K-Ar	Normal
P	0.59 ± 0.12	K-Ar	Normal
R	0.70 ± 0.06	K-Ar	Normal
K	0.95 ± 0.07	K-Ar	Reversed
CC	1.09 ± 0.05	K-Ar	Reversed

*Cation-ratio dating of rock varnish.

TABLE 2. CONE MORPHOMETRY

Cone	Age (m.y.)	Mean maximum slope angle S_c (°)	Tan S_c	Cone height: H_c (m)	Mean Cone width W_c (m)	H_c/W_c	Mean crater width W_{cr} (m)	W_{cr}/W_c	H_a/H_c	L_a/L_c
A	0.015	29.9	0.575	90	540	0.17	260	0.48	0.06	0.13
U	0.17	28.6	0.545	100	570	0.18	220	0.39	0.25	0.38
G	0.22	28.7	0.547	155	915	0.17	370	0.40	0.30	0.35
BB	0.33	25.8	0.483	90	620	0.15	300	0.48	0.28	0.38
E	0.35	28.5	0.543	130	690	0.19	220	0.32	0.24	0.36
J	0.46	26.5	0.499	50	420	0.12	170	0.40	..	..
F	0.59	26.5	0.499	100	560	0.18	170	0.30	0.35	0.43
P	0.59	23.5	0.435	95	650	0.15	190	0.29	0.32	0.39
R	0.70	24.0	0.445	100	570	0.17	..	..	..	..
K	0.99	22.1	0.406	75	630	0.12	130	0.21	0.35	0.38
CC	1.09	22.9	0.422	60	400	0.15	..	..	..	..

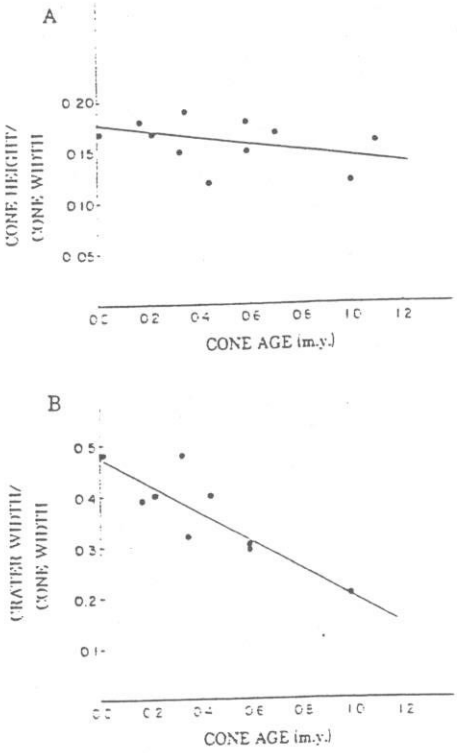

Figure 4. Variation of cone morphometry with time. A. Cone-height/cone-width ratios versus cone age. $H_c/W_c = 0.174 - 0.028\ t$ (t in m.y.); correlation coefficient = 0.403. B. Crater-width/cone-width ratios versus cone age. $W_{cr}/W_c = 0.474 - 0.270\ t$ (t in m.y.); correlation coefficient = 0.859. Refer to Table 2 for data values.

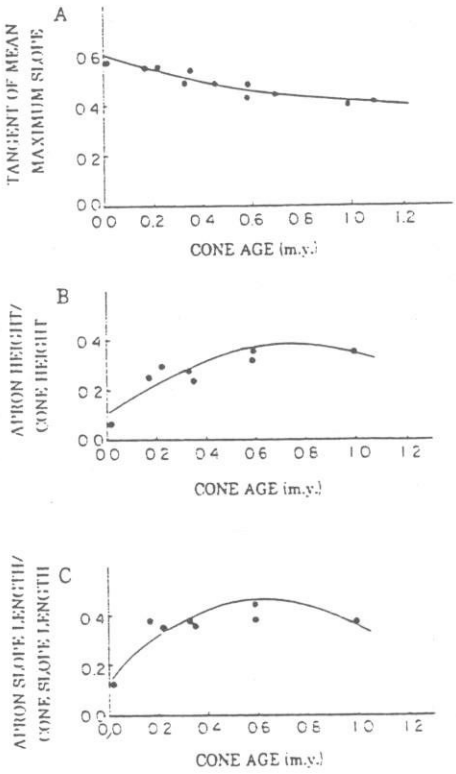

Figure 5. Variation of cone morphometry with time. A. Tangent of mean maximum cone slope versus cone age. Tan $S_c = 0.585 - 0.241\ t + 0.732\ t^2$ (t in m.y.); correlation coefficient = 0.927. B. Apron-height/cone-height ratios versus cone age. $H_a/H_c = 0.100 + 0.692t - 0.456\ t^2$ (t in m.y.); correlation coefficient = 0.891. C. Apron-slope-length/cone-slope-length ratios versus cone age. $L_a/L_c = 0.178 + 0.796\ t - 0.615\ t^2$ (t in m.y.); correlation coefficient = 0.873. Refer to Table 2 for data values.

generally increase with increasing age. H_c/W_c, decreasing from an average of ~0.17 for the younger cones to an average of ~0.14 for the oldest cones studied (Fig. 4A), shows a weakly defined inverse correlation with cone age. W_{cr}/W_c decreases from a maximum of 0.47 on the youngest cone to a minimum of 0.21 on the oldest cone with a preserved crater (Fig. 4B). Tan S_c decreases from a maximum of 0.575 on the youngest cone to an average of 0.414 on the oldest cones studied (Fig. 5A). H_a/H_c increases rapidly from a minimum of 0.06 on the youngest cone to a nearly constant maximum of 0.35 on cones 0.59 m.y. old and older (Fig. 5B). L_a/L_c follows a similar trend, increasing sharply from a minimum of 0.13 on the youngest cone to attain an apparent maximum of 0.41 on 0.59-m.y.-old cones (Fig. 5C). These systematic changes in morphology indicate a pattern of degradation dominated by (1) maximum erosion on upper cone slopes, reducing cone height and average slope, and (2) deposition of the eroded debris as aprons around lower cone slopes, increasing apparent cone width and further reducing the average slope. Erosion within cone craters undoubtedly also occurs; however, agglutinate armoring of crater walls and a lack of thick slope deposits within most craters suggest that this factor is relatively unimportant in the Cima field.

Qualitative morphologic evidence also indicates a general pattern of cone downwasting (Table 3). The sharp crests and well-defined craters of the younger cones gradually give way to the partly rounded crests and profoundly degraded craters of the older cones. On the oldest cones, the vestiges of craters survive only where a relatively resistant spatter-fed rootless flow or small crater-ponded flow remains to mark lower crater walls or floor. The depths of unbreached craters on the younger cones average ~25 m, and the absence of craters on most of the older cones suggests a comparable reduction in the heights of these older cones. The general lowering of outer cone slopes also argues strongly for a significant and progressive decrease in cone height over time.

Drainage Morphology

Progressive changes in cone height and slope morphology are accompanied by concomitant changes in drainage morphology (Fig. 6). The outer slopes of the youngest cone are only partly scarred by unevenly distributed rills and gullies. On 0.15- to 0.25-m.y.-old cones, numerous regularly spaced gullies occupy lower and middle cone slopes. Cones 0.30 to 0.35 m.y. old are marked by parasol-like patterns of straight, regularly spaced gullies that extend from the toe to the crest of most unbreached slopes. Mean gully cross-sectional areas on these younger cones (<0.4 m.y. old) remain relatively constant,

large surface drainage ways at the expense of both cone slopes and debris aprons; however, cone downwasting, as measured by either cone-height or slope-angle reduction, decreases to ~30% of initial rates.

It should be emphasized that this model is an empirical approximation and that it is subject to several sources of uncertainty. (1) The morphometric data used to develop the model were collected from a limited sample of 11 cones. (2) Significant morphologic variability occurs on several of these cones, and although most of this variability can be traced to identifiable external influences (for example, local burial by lava flows and/or pyroclastic debris, lateral fluvial erosion of cone flanks, eruptive breaching of cone flanks) and thus was excluded from model calculations, the useful sample size was further constrained. (3) Measured values of the various morphometric parameters are probably only significant to ±10% to 15%. Cone and apron boundaries are typically gradational, and many measurements were made from 1:24,000-scale, 10-m-contour maps and 1:20,000-nominal-scale, vertical aerial photographs. (4) Precision of the K-Ar ages of the various cones is also limited, the average 2-sigma error being about ±0.07 m.y. The rates and trends of cinder-cone degradation summarized in Figure 7 and Table 5 thus are approximations that are only generally applicable to other cinder-cone populations in arid and semiarid environments.

CONCLUSIONS

Cinder cones in the Cima volcanic field display progressive degradational changes that are closely related to cone age. (1) W_{cr}/W_c decreases from an average of 0.48 on the younger cones to 0.21 on the oldest cone with a preserved crater. (2) Tan S_c decreases from 0.575 on the youngest cone to ~0.41 on the oldest cones studied. (3) H_a/H_c increases from <0.10 on the youngest cone to an average of 0.34 on the oldest cones. (4) Drainage networks gradually evolve from widely scattered, irregularly spaced rills and small gullies on the youngest cone to small valleys as much as 110 m wide and 10 m deep on the oldest cones.

These morphologic trends indicate that, for the past million years at least, a primary mode of degradation of the Cima cinder cones has been general downwasting, a progressive decrease in cone height, and a concomitant decline in mean maximum slope. Profound degradation or complete elimination of craters on cones 0.7 m.y. and older substantiates this conclusion. Crater depths on the younger, unbreached cones average ~25 m, and the absence of craters on the older cones indicates a comparable reduction in cone height during the first 0.7 to 1.1 m.y. of cone degradation. This amount of height reduction is consistent with the decrease in cone height predicted by the cone-degradation model.

The cone-degradation model also provides a means to quantitatively estimate changes in cone volume, debris-apron volume, and drainage-way volume during the first million years of cone degradation. These changes include (1) an initially rapid and then more gradual downwasting loss totaling almost 15% of initial cone volume after the first million years; (2) an initially rapid but then decelerating increase in debris-apron volume that reaches a maximum of ~5.5% of initial cone volume after ~0.6 m.y.; and (3) an initially slow but gradually accelerating increase in drainage-way volume to almost 15% of initial cone volume after the first million years. Initial gains in debris-apron volume approximately offset downwasting losses, but after 0.15 to 0.25 m.y., the system opens, and total system losses increase to almost 15% of initial cone volume by the end of the first 1 m.y. of degradation.

Changes in the types and rates of degradational processes acting on the Cima cinder cones appear to be controlled primarily by changes in the structure and composition of materials exposed at the cone's surface by degradation and, to a much lesser extent, by external factors such as climatically induced changes in surficial processes. At any point in time, the general morphologic condition of each cone reflects the net effect, integrated over the cone's age, of all climatic changes that have occurred since the cone's formation. Consequently, an intelligible record of middle and late Pleistocene climatic change is not preserved in the progressive degradational morphology of the Cima cones; over the past million years, both cone heights and mean maximum cone slopes have declined uniformly despite several shorter term (10^4 to 10^5 yr) climatic fluctuations during this same time period.

Analysis of the degradational morphology of cinder cones is a potentially useful relative-age–dating tool for mapping volcanic fields and for assessing frequency and volumetric patterns of volcanic activity. Any relative dating scheme based on comparative degradational morphology should be field specific: it should be based on a representative sample of morphologic data collected from the volcanic field being studied and calibrated by a carefully selected series of radiometric age dates. Under these conditions, relative degradational morphology can be used to supplement radiometric dating. In arid and semiarid environments, age estimates based on relative degradational changes have a potential precision of approximately ±0.15 m.y.

ACKNOWLEDGMENTS

Reviewed by William B. Bull, Duane E. Champion, William J. Keith, Edward W. Wolfe, and Charles A. Wood; we appreciate their insightful comments and helpful suggestions. We also thank Jeanette Smith for assistance in the field.

REFERENCES CITED

Bloomfield, K., 1975, A late-Quaternary monogenetic volcano field in central Mexico: Geologische Rundschau, v. 64, p. 476–497.

Colton, H. S., 1967, The basaltic cinder cones and lava flows of the San Francisco Mountain volcanic field (revised edition): Flagstaff, Arizona, Museum of Northern Arizona, 56 p.

Dohrenwend, J. C., McFadden, L. D., Turrin, B. D., and Wells, S. G., 1984a, K-Ar dating of the Cima volcanic field, eastern Mojave Desert, California: Late Cenozoic volcanic history and landscape evolution: Geology, v. 12, p. 163–167.

Dohrenwend, J. C., Wells, S. G., Turrin, B. D., and McFadden, L. D., 1984b, Rates and trends of late Cenozoic landscape degradation in the area of the Cima volcanic field, Mojave Desert, California, *in* Dohrenwend, J. C., ed., Surficial geology of the eastern Mojave Desert, California: Geological Society of America 1984 Annual Meeting Guidebook, p. 101–115.

Dorn, R. I., 1984, Geomorphological interpretation of rock varnish in the Mojave Desert, *in* Dohrenwend, J. C., ed., Surficial geology of the eastern Mojave Desert, California: Geological Society of America 1984 Annual Meeting Guidebook, p. 150–161.

Embleton, C., and Thornes, J., 1979, Sub-surface processes, *in* Embleton, C., and Thornes, J., eds., Process in geomorphology: New York, John Wiley and Sons, p. 187–212.

Harland, W. B., Cox, A. V., Llewellyn, P. G., Pickton, C.A.G., Smith, A. G., and Walters, R., 1983, A geologic time scale: Cambridge, England, Cambridge University Press, 131 p.

Hasenaka, T., and Carmichael, I.S.E., 1985, The cinder cones of Michoacan-Guanajuato, central Mexico: Their age, volume and distribution, and magma discharge rate: Journal of Volcanology and Geothermal Research, v. 25, p. 105–124.

Kear, D., 1957, Erosional stages of volcanic cones as indicators of age: New Zealand Journal of Science and Technology, v. 38B, p. 671–682.

McFadden, L. D., Wells, S. G., Dohrenwend, J. C., and Turrin, B. D., 1984, Cumulic soils formed in eolian parent materials of flows of the Cima volcanic field, Mojave Desert, *in* Dohrenwend, J. C., ed., Surficial geology of the eastern Mojave Desert, California: Geological Society of America 1984 Annual Meeting Guidebook, p. 134–145.

Porter, S. C., 1972, Distribution, morphology, and size frequency of cinder cones on Mauna Kea Volcano, Hawaii: Geological Society of America Bulletin, v. 83, p. 3607–3612.

Scott, D. H., and Trask, N. J., 1971, Geology of the Lunar Crater Volcanic Field, Nye County, Nevada: U.S. Geological Survey Professional Paper 599-I, 22 p.

Settle, M., 1979, The structure and emplacement of cinder cone fields: American Journal of Science, v. 279, p. 1089–1107.

Turrin, B. D., Dohrenwend, J. C., Wells, S. G., and McFadden, L. D., 1984, Geochronology and eruptive history of the Cima volcanic field, eastern Mojave Desert, California, *in* Dohrenwend, J. C., ed., Surficial geology of the eastern Mojave Desert, California: Geological Society of America 1984 Annual Meeting Guidebook, p. 86–100.

Wells, S. G., Dohrenwend, J. C., McFadden, L. D., Turrin, B. D., and Mahrer, K. D., 1984, Types and rates of late Cenozoic geomorphic processes on lava flows of the Cima volcanic field, Mojave Desert, California, *in* Dohrenwend, J. C., ed., Surficial geology of the eastern Mojave Desert, California: Geological Society of America 1984 Annual Meeting Guidebook, p. 116–133.

Williams, H., and McBirney, A. R., 1979, Volcanology: San Francisco, California, Freeman, Cooper and Company, 397 p.

Wood, C. A., 1980a, Morphometric evolution of cinder cones: Journal of Volcanology and Geothermal Research, v. 7, p. 387–413.

——1980b, Morphometric analysis of cinder cone degradation: Journal of Volcanology and Geothermal Research, v. 8, p. 137–160.

Manuscript Received by the Society June 3, 1985
Revised Manuscript Received October 23, 1985
Manuscript Accepted October 25, 1985

Printed in U.S.A.

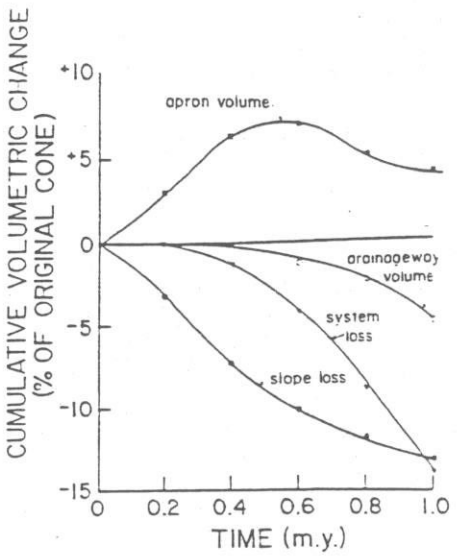

Figure 7. Degradation of an "average" Cima cone over the first million years. Cumulative volumetric change (expressed as % of original cone volume) versus time. Refer to Table 5 for values of the volume estimates expressed as 10^5 m^3 and as percentage of original cone volume. Refer to Table 4 for the values of the morphometric parameters used to calculate these volume estimates.

most complete absence of tectonic activity (Dohrenwend and others, 1984a, 1984b). The present condition of cones of different ages, therefore, can be considered to represent different stages in the degradation of a single cone in a generally downwasting, tectonically quiescent environment.

2. The foregoing assumption implies that the erosional morphology of the Cima cones has been relatively insensitive to Quaternary climatic variations. The present form of each cone undoubtedly reflects the cumulative effects of several significant middle to late Pleistocene climatic fluctuations; however, the effects of any one change have been overprinted and obscured by tens to hundreds of thousands of years of subsequent erosion and by the effects of all succeeding climatic changes. The degradational changes exhibited by the Cima cones are progressive and do not preserve a sensitive record of climatic fluctuation.

3. Mean maximum slopes (Tan S_c), apron-height/cone-height ratios (H_a/H_c), apron-slope-length/cone-slope-length ratios (L_a/L_c), and drainage characteristics of the 11 dated cones are representative of all cinder cones in the Cima field (excluding cones associated with tephra rings).

TABLE 4. MODEL OF CONE DEGRADATION: SIGNIFICANT PARAMETERS

Time (m.y.)	Mean cone slope angle S_c (°)	Mean cone slope Tan S_c	H_a/H_c	L_a/L_c	Apron height H_a (m)	Cone height H_c (m)	Mean apron slope angle S_a (°)	Mean apron slope Tan S_a
0.0	30.5	0.590	..	..	0.0	100.0	..	..
0.2	28.7	0.547	0.24	0.35	22.5	95.5	16.0	0.288
0.4	26.2	0.492	0.30	0.40	26.5	88.5	16.4	0.294
0.6	24.4	0.454	0.34	0.42	28.5	84.5	16.9	0.304
0.8	23.2	0.429	0.36	0.40	29.5	81.5	20.1	0.366
1.0	22.5	0.414	0.37	0.38	29.5	79.5	21.8	0.399

TABLE 5. MODEL OF CONE DEGRADATION: CUMULATIVE EROSION EXPRESSED IN PERCENTAGE OF CONE VOLUME

Time (m.y.)	Downwasting loss		Drainage-way volume		Debris-apron volume		Total system loss	
	10^5 m^3	%	10^5 m^3	%	10^5 m^3	%	10^5 m^3	%
0.2	−4.8	−3.5	−0.03	−0.02	+5.1	+3.7	+0.3	+0.2
0.4	−10.2	−7.4	−0.4	−0.3	+6.7	+4.9	−3.9	−2.8
0.6	−13.6	−9.9	−1.6	−1.2	+7.5	+5.5	−7.7	−5.6
0.8	−16.0	−11.6	−3.1	−2.3	+5.2	+3.8	−13.9	−10.1
1.0	−17.6	−12.8	−6.4	−4.7	+3.9	+2.9	−20.1	−14.6

The initial condition for this empirical model is an unbreached, undissected cone that approximates a truncated right, circular cone in over-all form. The dimensions of this initial cone closely approximate the average dimensions of the youngest Cima cones: H_c = 100 m; W_c = 590 m; H_c/W_c = 0.17; W_{cr}/W_c = 0.42; and S_c = 30.5° (Tan S_c = 0.590).

To determine the volumetric change of this initial cone during the first million years of degradation, values of S_{ct}, $(H_a/H_c)_t$, and $(L_a/L_c)_t$ were estimated for 0.2-m.y. intervals from the plots in Figure 5 (Table 4, columns 2–5). H_{at} (apron height at time t) and H_{ct} (cone height at time t) were then calculated from the following two relations:

$$\text{Sin } S_{ct} = (H_{ct} - H_{at}) / (L_{ct} - L_{at}) \qquad (1)$$

and

$$\text{Tan } S_{ct} = (H_{ct} - H_{at}) / [((W_{co} - W_{cro}) /2) - (H_{at} / \text{Tan } S_{co})], \qquad (2)$$

where S_{ct} is the cone slope angle at time t, S_{co} is the cone slope angle at time t = 0, W_{co} is the cone width at time t = 0, and W_{cro} is the crater width at time t = 0. (Equations 1 and 2 are derived from the geometric relations shown in Fig. 2.) Values of H_{at} and H_{ct} are listed in Table 4, columns 6 and 7. S_{at} (average apron slope angle at time t) was calculated from the relation:

$$\text{Sin } S_{at} = H_{at}\text{Sin } S_{ct} / \{(H_{ct} - H_{at})[(L_{at} / L_{ct}) / (1-(L_{at} / L_{ct}))]\}. \qquad (3)$$

(Equation 3 results from an algebraic rearrangement of equation 1 to solve for L_{at} and substitution of the resulting expression into the equation, Sin S_{at} = H_{at}/L_{at}.) Values of S_{at} are listed in Table 4, columns 8 and 9.

The dimensions of the initial undissected cone and values of H_{ct}, H_{at}, S_{ct}, and S_{at} from Table 4 were used in volumetric calculations of the appropriate combinations of truncated, right, circular cones to estimate the amount of material removed from the cone slope and deposited in the surrounding debris apron for each 0.2-m.y. interval. In addition, estimates of drainage-way volume at the end of each 0.2-m.y. interval were approximated from measurements of drainage-way dimensions on several of the Cima cones. Cumulative totals of all of these estimates, expressed in terms of the percent of volume of the initial undissected cone, are listed in Table 5.

Comparison of the changes in cone volume, drainage-way volume, and debris-apron volume over the first million years of cone degradation is facilitated by Figure 7. During the first 0.15 to 0.25 m.y., loss of cone material, mainly from crestal and upper-slope areas, approximately equals debris-apron gains. H_a/H_c and L_a/L_c ratios increase rapidly during this period (Fig. 5). During the next 0.3 to 0.4 m.y., this approximate balance between cone erosion and apron growth gradually gives way. Debris aprons grow more slowly, stop growing, and finally decrease in size. H_a/H_c and L_a/L_c ratios increase slowly during this time. The peaking of debris-apron growth signals completion of stripping of the loose cinder mantle from upper cone slopes and initiation of large-gully and small-valley erosion as surface-wash processes become established on the less pervious materials of the cone interior. During the final 0.4 m.y., total system losses accelerate as fluvial processes continue to en-

however; gully depths average between 0.4 and 0.5 m, and gully widths average between 1.5 and 2.5 m. In contrast, gullies on older cones are larger, are more widely spaced, and intersect more frequently. Gully cross-sectional areas average as much as five times the mean cross-sectional areas of gullies on the younger cones. On cones 0.59 m.y. old and older, these larger gullies feed second-order valleys that are as much as 10 m deep, 110 m wide, and 200 m long.

Initial development of gullies on the Cima cones appears to be strongly influenced by debris-flow processes. Most gullies on the youngest Cima cone are characterized by channels with approximately parabolic cross sections and 0.2- to 0.4-m-high levees of pebble- to cobble-sized cinders. Several of these channels terminate abruptly in lower mid-slope above the base of the cone, and conspicuous, lobate masses of poorly sorted cone debris extend beyond the downslope ends of these channels. The mid-reaches of many other channels are partly filled with smaller debris lobes and/or lobate sieve deposits. Similar relations exist on all of the younger dated cones at Cima. The abundance and wide distribution of these features on the younger cones suggest that debris-flow processes are significant in the early stages of degradation of the Cima cones. The similarity in form and mean cross-sectional area of gullies on cones younger than 0.4 m.y. and the existence of many partly filled gully channels suggest a general scenario of channel excavation by large debris-flow events, followed by gradual channel burial beneath smaller debris-flow lobes and sieve deposits. Repeated channel excavation and filling apparently continue until the bulk of the pervious cinder mantle is removed and concentrated surface-water flow is established across the relatively impervious materials of the cone interior. This process provides a plausible explanation for significant cone-height reduction preceding the formation of large surface drainage ways.

TABLE 3. QUALITATIVE DESCRIPTION OF CONE DEGRADATION

Cone	Age (m.y.)	Morphologic characteristics
A	0.015	Sharp crest; well-defined crater; 30°–35° slopes; debris aprons very narrow to absent; unevenly distributed rills and small gullies; prominent garlands.*
U G	0.17 0.25	Sharp to moderately sharp crest; well-defined crater; 28° to 30° slopes; narrow debris aprons; evenly spaced gullies occupy middle and lower parts of slopes; prominent garlands.
EE BB E	0.27 0.33 0.35	Sharp to moderately sharp crest; well-defined crater; 25° to 29° slopes; fully developed debris aprons; evenly spaced gullies extend from toe to crest of most slopes; garlands indistinct or absent.
F P	0.59 0.59	Moderately sharp to partly rounded crest; extensively degraded crater, internal structures exposed; 24° to 27° slopes; irregular, degraded debris aprons, larger, more widely spaced gullies; appearance of small valleys.
R K CC	0.70 1.00 1.09	Partly rounded crest; crater extensively degraded or absent; internal structures control cone form; 22° to 24° cinder-covered slopes; second-order drainage in valleys as much as 110 m wide.
P	3.00	Internal structures dominate vent form.

*Subhorizontal bands of cobble-sized tephra fragments; these bands are as much as 5 m wide, curvilinear in planform, and generally convex downslope.

Piping may also contribute to gully development on the Cima cones. This process is common in areas with steep hydraulic gradients underlain by noncohesive materials of variable permeability, particularly where pervious horizons are interbedded with less pervious horizons (Embleton and Thornes, 1979). The uppermost 0.3 to 0.5 m of the cinder mantle on the Cima cones is commonly impregnated with eolian silt. This silt is irregularly distributed. Ponded silt at least several metres thick occurs in unbreached craters, cinder pavements underlain by at least 0.3 m of relatively cinder-free silt occur on the crests of some of the older cones, and irregular zones of partial silt impregnation are exposed in gullies and road-cuts on cone flanks. Beneath this silt-rich surface, the cinder mantle is relatively silt-free, and piping is common. Pipes exposed in road-cuts across cone slopes are as much as 0.5 m wide, 0.3 m high, and several metres long. Pipe formation at gully heads and upslope migration of pipe collapse thus are likely mechanisms of gully elongation on the younger Cima cones.

In summary, erosion of the cone crest and upper slopes begins with broadly distributed and relatively uniform stripping of the loose cinder mantle by intermittent debris flow, pipe flow and diffuse subsurface water flow, and limited surface water-flow processes. Over time, this relatively uniform stripping via a parasol-like network of shallow, straight, nonbifurcating gullies is gradually concentrated into a radial network of small valleys fed by deep, bifurcating, tributary gullies. This transition is apparently controlled by a change in the hydrogeologic characteristics of the eroding substrate, from a pervious mantle of loose pyroclastic debris to a relatively impervious framework of agglutinate and flow rock that forms erosion-resistant cores within most cones.

MODEL OF CONE DEGRADATION

The progressive morphologic changes in the Cima cones and the relations between the various morphometric parameters used to quantify these changes permit quantitative description of cone erosion and debris-apron construction over the past 1 m.y. (Fig. 7; Tables 4 and 5). This model is based upon three major assumptions.

1. Age is the only factor that varies significantly among the Cima cones, and, therefore, time is the only factor that significantly affects the progressive morphologic changes exhibited by these cones. The Cima cones are all of similar composition and structure, and they are all situated in a more or less uniformly downwasting erosional environment characterized by an al-

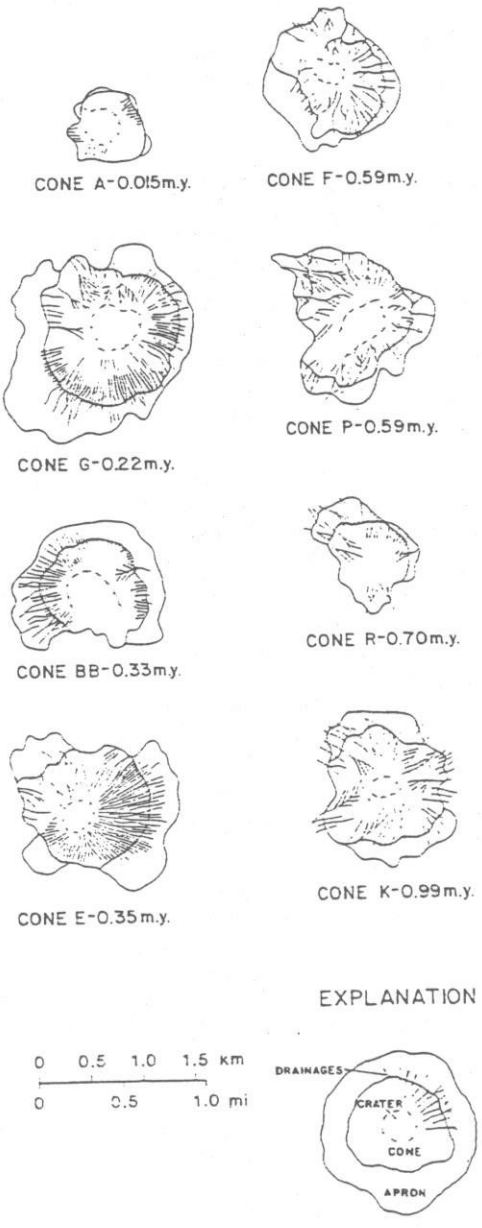

Figure 6. Drainage network development on dated Cima cones. Refer to Figure 2 for cone locations.